Solid State Science and Technology, Vol. 33, No. 1 (2025) 44-54
https://doi.org/10.66514/ssst33-1-44-54

Measurement and Numerical Simulation of Transmission and Reflection Characteristics of Recycled Hematite/OPEFB Fiber/Polycaprolactone Nanocomposites using Microstrip Line and Finite Element Method

Ebenezer Ekow Mensah[1,2,], Raba'ah Syahidah Azis[1,3,]*, Zulkifly Abbas[4]*

[1]Department of Physics, Faculty of Science, Universiti Putra Malaysia, 43400 Serdang Selangor, Malaysia

[2]Department of Integrated Science Education, Faculty of Science Education, Akenten Appiah-Menka University of Skills Training and Entrepreneurial Development, P. O. Box 40, Mampong-Ashanti, Ghana

[3]Materials Synthesis and Characterization Laboratory (MSCL), Institute of Nanoscience and Nanotechnology, Universiti Putra Malaysia, 43400 UPM Serdang, Selangor, Malaysia

[4]Xiamen University Malaysia, Jalan Sunsuria, Bandar Sunsuria, 43900 Sepang Selangor, Malaysia

**Corresponding authors: ebemensek@yahoo.co.uk, rabaah@upm.edu.my*

(Received: 25 March 2025 / Revised: 10 June 2025 / Accepted: 18 June 2025 / Published online: 24 June 2025)

ABSTRACT

Recycled hematite/OPEFB fiber/polycaprolactone nanocomposites were fabricated for microwave absorbing applications in the 1 – 4 GHz range. The aim of the study was to compare the magnitudes of the measured and simulated transmission (S_{21}) and reflection (S_{11}) parameters of the nanocomposites using the microstrip line technique and the Finite Element Method (FEM), since accurate measurement of electromagnetic parameters is essential for assessing the attenuation performance of microwave absorbing materials. The FEM simulation was carried out on COMSOL Multiphysics® version 5.2 and was based on the geometry of the microstrip used for the measurements. The comparison showed that the FEM-simulated S_{21} and S_{11} profiles closely matched the measured by a mean relative error of 20.6 % for S_{11} and 1.9 % for S_{21}, indicating a good agreement between both techniques. Hence, the microstrip technique for the measurement of transmission coefficient magnitudes provides a more reliable solution for characterizing the microwave absorption properties of the nanocomposites in the stated frequency range.

Keywords: Recycled hematite; Finite Element Method; Scattering Parameters; OPEFB Fiber

INTRODUCTION

The electromagnetic interference (EMI) phenomenon confronting electronic systems with civilian and military applications operating in the microwave frequency range has attracted solutions from several researchers aimed at improving the quality and reliability of such devices. For effective EMI absorption, materials must possess the right mixture of low density, low cost, electrical performance, thinness, mechanical properties, broadband applications [1,2] and biodegradability.

In the last few years, much attention has been directed towards the use of ferrite materials (spinel, garnet and hexagonal ferrites) for microwave absorption in view of their outstanding saturation magnetization, lowered electrical losses, considerable electrical resistivity and chemical stability. In this regard, ferrites including zinc ferrite [3], cobalt ferrite [4], magnetite [5] and La – Ni substituted barium ferrite [6], have been incorporated into composites which have demonstrated enhanced absorption covering a wide range of microwave frequency. As a result of the apparent high precursor, synthesis, equipment and solvent costs [7,8] of ferrite materials, carbon bio-based materials and low-cost recycled hematite (α-Fe_2O_3) used in conjunction with biodegradable polymeric materials have been suggested as suitable alternatives in previous works [9-11] , after analyzing their microwave absorption properties through measurements of the complex relative permittivity and permeability properties as well as their reflection and transmission coefficients or scattering parameters.

Considering the importance of scattering parameters in describing the interactions between electromagnetic waves and materials, their accurate measurement and prediction is key to assessing the absorbing characteristics of the materials. In this regard, a wide range of numerical solutions such as method of moment (MoM), finite difference time – domain method (FDTD) and finite element method (FEM) are available to model these interactions [12]. In this work, the scattering parameters of recycled hematite/OPEFB fiber/polycaprolactone nanocomposites were measured in the 1-4 GHz range using the microstrip line technique. Subsequently, the Finite Element Method, based on the microstrip model geometry, was also used to simulate the scattering parameters for the nanocomposites in the same frequency range similar to the study by Kim et al. [13]. The aim was to compare the results obtained through measurement and simulation.

Microwave absorbers need to be lighter and also possess high imaginary (ε'') part of complex relative permittivity so as to achieve higher absorbing characteristics. With OPEFB fiber of reduced grain size having a high ε'', its incorporation into recycled hematite/polycaprolactone blend could provide the desired outcome, while keeping the magnetic properties of the nanocomposites. Additionally, it is biodegradable and cheap, and its low density could also make the nanocomposites lighter.

Since numerical methods are more precise, a good agreement with measurements could indicate the accuracy and reliability in the determination and prediction of the absorbing performance of the materials under study. Furthermore, the simulation could aid in minimizing fabrication cost since only nanocomposites possessing optimum absorption characteristics would be fabricated.

MATERIALS AND METHODS

Synthesis of recycled hematite/OPEFB fiber/polycaprolactone nanocomposites

A 16.2 nm recycled hematite (α-Fe_2O_3) was synthesized from mill scale waste using procedures outlined in Mensah et al. [9]. Portions of 5 to 25 %wt. of the recycled α-Fe_2O_3 were subsequently mixed with various %wt. PCL (Sigma-Aldrich, St. Louis, MO, USA) and OPEFB fiber (grain size =100 μm) in a Brabender Extruder (Brabender GmbH & Co. KG, Duisburg, Germany) according to Table 1 to synthesize the nanocomposites. A fixed mixing ratio of 3:7 for PCL and OPEFB fiber was respectively applied to ensure that more fiber was utilized while the Brabender maintained its capacity to melt-blend the materials uniformly. Each of the nanocomposites was then placed into 6 cm × 3.6 cm × 0.20 cm molds and hot-pressed at a pressure of 110 kg/cm^2 into flat blocks.

Table 1. Composition of $(\alpha\text{-}Fe_2O_3)_x (PCL)_{0.3(100-x)} (OPEFB)_{0.7(100-x)}$ samples

α-Fe_2O_3		**PCL**		**OPEFB**		**Total Mass**
(*x* %)	Mass ± 0.0005 g	0.3(100-x) %	Mass ± 0.0005 g	0.7(100-x) %	Mass ± 0.0005 g	± 0.0005 g
5.0	1.2500	28.5	7.1200	66.5	16.6300	25.0000
10.0	2.5000	27.0	6.7500	63.0	15.7500	25.0000
15.0	3.7500	25.5	6.3800	59.5	14.8700	25.0000
20.0	5.0000	24.0	6.0000	56.0	14.0000	25.0000
25.0	6.2500	22.5	5.6300	52.5	13.1200	25.0000

Characterizations - Structure and Composition

The structure, phase composition and formation of the recycled hematite and nanocomposites were investigated using Xray diffraction (XRD) technique on a Philips X-pert system (Model PW3040/60 MPD, Amsterdam, The Netherlands) of Cu-Kα radiation with respective operational voltage, current and wavelength of 40.0 kV, 40.0 mA 1.5405 Å. The diffraction patterns were taken in the 2-theta range of 10–80° using a scanning speed of 2 °/min. All data were run through Rietveld analysis using PANalytic X'Pert Highscore Plus version 3.0 software (PANalytical B.V., Almelo, The Netherlands). The recycled hematite sample was identified by matching the diffraction patterns with Inorganic Crystal Structure Database (ICSD).

Measurement of Complex Permittivity

The real (ε) and imaginary (ε'') parts of complex relative permittivity characteristics of the samples were determined from Agilent 85070B open ended coaxial (OEC) probe measurements in conjunction with Agilent N5230A PNA-L Vector Network Analyzer (Agilent Technologies, California, U.S.A.). Measurements were made at room temperature and in the 1–4 GHz frequency range by placing the OEC probe onto the flat and smooth surfaces of the materials while ensuring that was no air-gap between the contact surfaces. In the case of the recycled hematite, the nanopowders were compressed into a sample holder with a 2.5 cm top diameter, 2 cm base diameter a height of 3 cm. The variations in ε and ε'' with recycled hematite nanofiller content at selected frequencies were subsequently examined.

Measurement of Scattering Parameters

The magnitudes of the reflection coefficient (S_{11}) and transmission coefficient (S_{21}) of the recycled hematite/OPEFB fiber/polycaprolactone nanocomposites were determined from the transmission/reflection line method which was based on the R-T duriod 5880 microstrip with a signal line of dimensions 6.0 cm × 0.15 cm engraved along its wider side. The microstrip had a width of 5.0 cm, length 6.0 cm, thickness 0.15 cm and was connected to a two-port Anritsu MS 2024B VNA Master (Anritsu Corporation, Kanagawa, Japan). After performing a standard calibration of short, open and load, measurements were subsequently performed at 1-4 GHz frequency range by placing the nanocomposites flat onto the microstrip surface while ensuring an air-gap free contact with the strip line for accurate data acquisition. The variation in S_{11} and S_{21} magnitudes with frequency range of measurement was then investigated.

The simulated values of the scattering parameters were theoretically determined using FEM performed on COMSOL Multiphysics software version 5.2 (COMSOL AB, Stockholm, Sweden) based on the R-T duriod 5880 microstrip geometry. The procedure consisted of creating the model geometry, defining physical parameters and boundary conditions followed by meshing the model geometry which was subsequently solved. The measured permittivity values of the nanocomposites were used as inputs for the software and the S_{11} and S_{21} magnitudes were extracted after performing parametric studies on the results of the simulation. The variation in calculated S_{11} and S_{21} magnitudes with frequency range of measurement was also determined. Figure 1 shows created model of the microstrip.

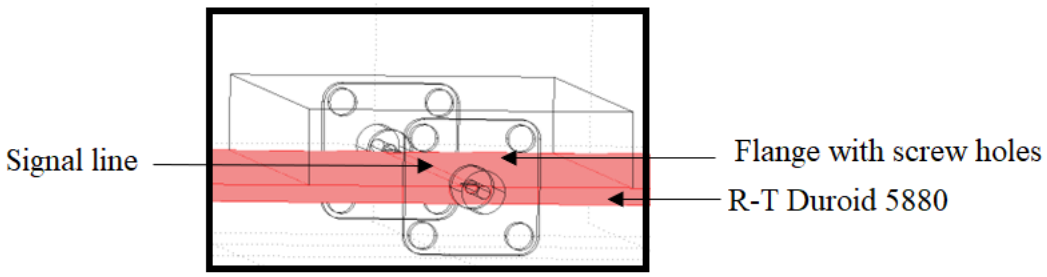

Figure 1. FEM generated model of the microstrip

RESULTS AND DISCUSSION

Structure and Composition

The confirmation of the synthesis of recycled hematite from mill scale and its nanostructure characterization was extensively reported in our previous work [14]. Figure 2 shows the X-ray diffraction patterns of the α-Fe_2O_3/OPEFB fiber/PCL nanocomposites where the broad peak representing cellulose crystallinity within the OPEFB fiber is clearly noticeable at 22.4º [15]. Additionally, the diffraction patterns also show the presence of the maximum intensity peaks belonging to α-Fe_2O_3 and PCL consistent with previous studies [11,16,17]. It is therefore evident that the patterns comprise the main intensity peaks of recycled α-Fe_2O_3 nanopowders, PCL polymer matrix and OPEFB fiber. The significant absence of any changes in the peak positions or the formation of new

peaks suggests that there is a weak interaction between recycled α-Fe_2O_3 nanopowders, PCL polymer matrix and the OPEFB fiber. Therefore, the melt-blending of these materials to synthesize the nanocomposites was physical in nature and resulting properties exhibited reflect those of the individual constituents of the nanocomposites.

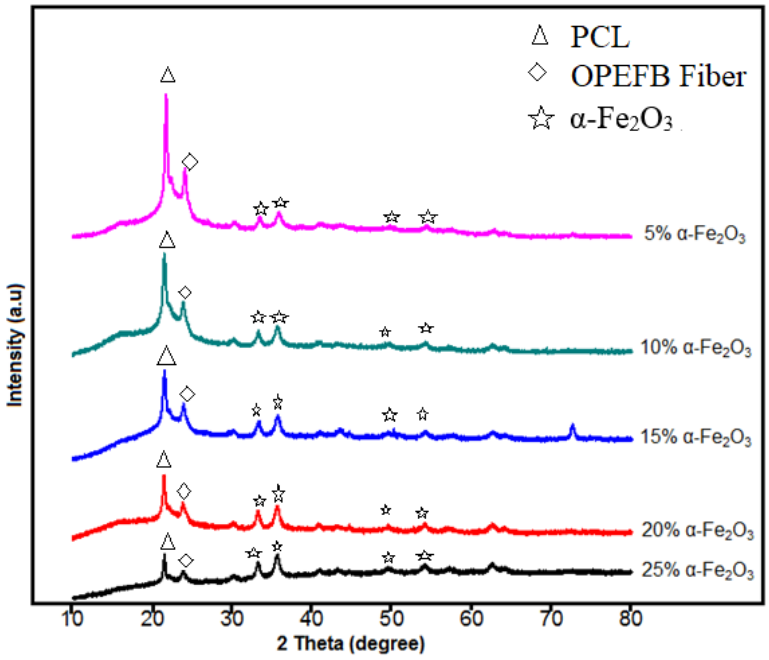

Figure 2. XRD diffractograms of α-Fe_2O_3/OPEFB/PCL nanocomposites

Complex Permittivity

Figures 3 and 4 indicate linear variations in ε and ε'' with recycled hematite nanofiller content at selected frequencies. A close observation of Figure 3 shows a general decrease in ε with frequency within the 1 GHz to 4 GHz frequency range whereas the ε'' values depicted in Figure 4 rather increased with frequency at the same nanofiller content to a maximum of 0.63 at 4 GHz. This is significant since materials with high ε'' are preferable as they are predicted to absorb more electromagnetic energy[18]. However, both figures demonstrated increases in permittivity values with nanofiller content at the selected frequencies in accordance with the results of previous research [19,20].

This could be attributed to the reduction in the inter-particle distance of the nanofiller as its quantity in the polymer matrix increased leading to a decrease in charge trapping centers and probability of charge nullification resulting in the permittivity values increasing as nanofiller increased. Moreover, the addition of OPEFB fiber into the PCL matrix improved the major mechanism of orientation and interfacial polarization which resulted in the observed increase in the permittivity values [21].

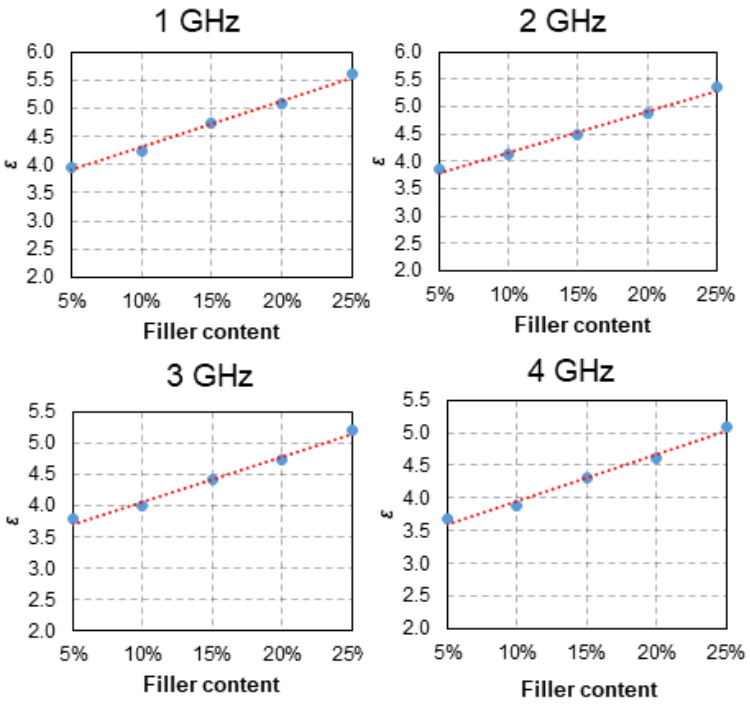

Figure 3. Variation in ε with respect to filler content at selected frequencies

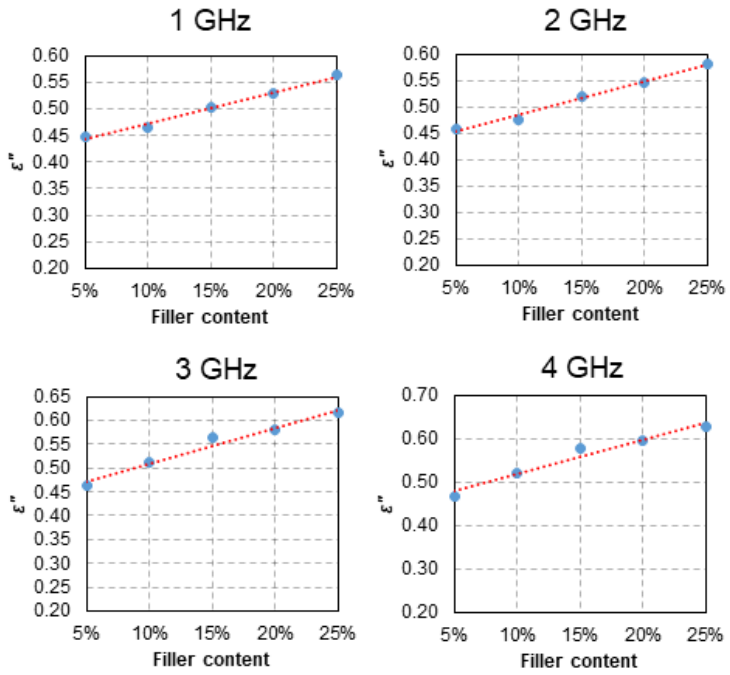

Figure 4. Variation in ε'' with respect to filler content at selected frequencies

Scattering Parameters

The comparison between the measured and simulated S_{11} magnitudes for the α-Fe_2O_3/OPEFB fiber/PCL nanocomposites is presented in Figure 5 in which evidently, the minimum and maximum magnitudes of the parameters coincide at the same frequencies

indicating a good agreement between both techniques with increasing recycled α-Fe_2O_3 nanofiller content. However, the significant deviation between the two methods beyond 2.5 GHz can be ascribed to several factors which the simulation process did not consider. The FEM simulations presumed ideal conditions including the absence of stray radiation and reflections between connectors and samples. But with real measurements, multiple reflections with losses together with stray radiation at the boundary between the nanocomposites and the microstrip's SMA launcher could not be averted. The multiple-reflections effect at the anterior and posterior surfaces of the nanocomposites, increased with frequency resulting in the noticeable high deviations in the FEM simulations. Again, the SMA launcher had a 6 mm x 6 mm metal square panel which was much smaller than the nanocomposites' thickness causing reduced contact which led to the deviations. Additionally, the computational precision of FEM largely depended on the accuracy of the processing software's auto generated mesh dimensions typically at the interface between the launcher and sample.

Figure 6 also shows that the S_{21} magnitudes calculated by FEM decreased with an increase in recycled α-Fe_2O_3 nanofiller content as frequency increased, consistent with the measurement results. This indicates good agreement between the measured and simulated S_{21} magnitudes for the α-Fe_2O_3/OPEFB fiber/PCL nanocomposites. It can clearly be observed that FEM simulated the profiles of the parameters closely with those of the measured, however, differences in the magnitudes emerged because of factors assumed ideal in the simulation procedure. Moreover, as the recycled hematite nanofiller content increased in the nanocomposites, a much better agreement between the measured and the calculated parameters developed due to the increase in ε'' values.

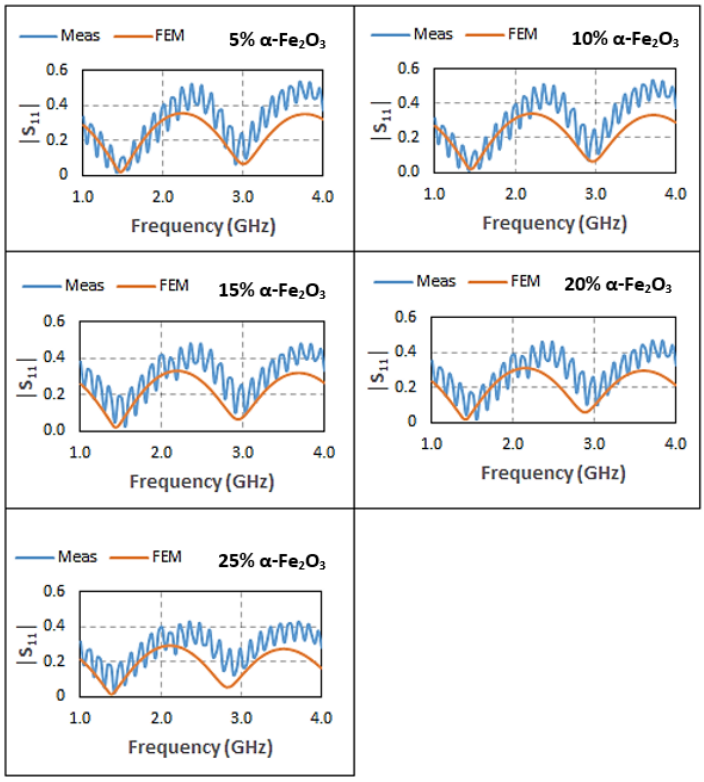

Figure 5. Comparison of S_{11} magnitudes determined from Measurements and FEM

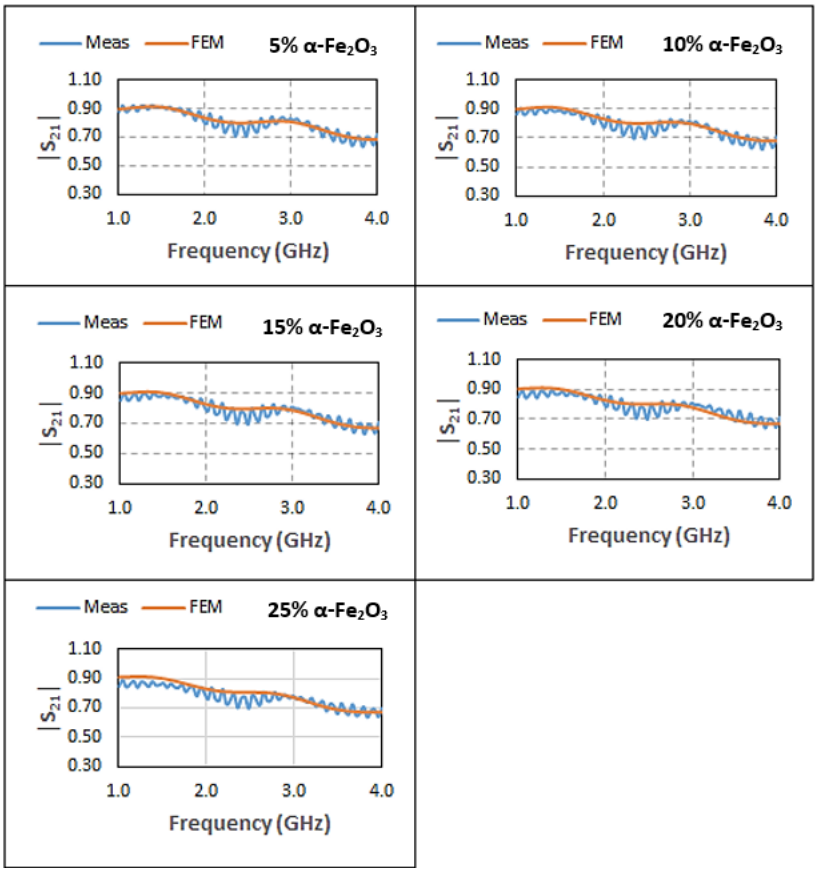

Figure 6. Comparison of S_{21} magnitudes determined from Measurements and FEM

The relative errors listed in Table 2 suggest that the 5% and 20% α-Fe_2O_3/OPEFB fiber/PCL nanocomposites obtained both the lowest $|S_{11}|$ and $|S_{21}|$ relative error of 0.107 and 0.009 respectively. Therefore, the mean relative error between the two measurement techniques were found to be 20.6 % for reflection coefficient magnitudes and 1.9 % for transmission coefficient magnitudes. This confirms the better agreement between measurement and FEM for transmission coefficient magnitudes as illustrated in Figure 6.

Table 2. Mean relative error in $|S_{11}|$ and $|S_{21}|$ between measurement and FEM for α-Fe_2O_3/OPEFBfiber/PCL the nanocomposites

	Relative Error	
α-Fe_2O_3	S_{11}	S_{21}
5%	0.107	0.013
10%	0.108	0.028
15%	0.327	0.017
20%	0.196	0.009
25%	0.291	0.030
Mean	0.206	0.019

CONCLUSION

In this study, the fabricated recycled hematite/OPEFB fiber/PCL nanocomposites were characterized by measuring their complex permittivity properties and scattering parameters in the 1-4 GHz frequency range. The scattering parameters were measured with the aid of the microstrip technique and also theoretically calculated using the finite element method (FEM) based on the model geometry of the microstrip. A comparison between measured and simulated scattering parameters was made to ascertain the accuracy and reliability of the measurement technique since numerical methods are more precise.

These results showed linear variations in ε and ε'' with recycled hematite nanofiller content at selected frequencies. The ε'' values increased with frequency at the same nanofiller content to a maximum of 0.63 at 4 GHz. The comparison between FEM-simulated S_{21} and S_{11} profiles and measured S_{21} and S_{11} closely matched by a mean relative error of 20.6 % for S_{11} and 1.9 % for S_{21}, indicating a good agreement between both techniques. Hence, the microstrip technique for the measurement of transmission coefficient magnitudes provides a more reliable solution for characterizing the microwave absorption properties of the recycled hematite/OPEFB fiber/PCL nanocomposites in the stated frequency range.

FUNDING STATEMENT

This work supported is by the Ministry of Higher Education, Malaysia under the Fundamental Research Grants Scheme (FRGS), (FRGS/1/2023/STG07/UPM/02/8).

DECLARATION OF INTEREST STATEMENT

The authors declare no conflict of interest.

ACKNOWLEDGEMENTS

The authors wish to thank the Department of Physics, Faculty of Science, Universiti Putra Malaysia and Materials Synthesis and Characterization Laboratory (MSCL), Institute of Nanoscience and Nanotechnology, Universiti Putra Malaysia for providing the measurement facilities.

REFERENCES

1. Liu X, Wu J, He J, Zhang L. Electromagnetic interference shielding effectiveness of titanium carbide sheets. *Mater Lett*. 2017;205:261–3. doi:10.1016/j.matlet.2017.06.101.
2. Shen P, Luo J, Zuo Y, Yan Z, Zhang K. Effect of La-Ni substitution on structural, magnetic and microwave absorption properties of barium ferrite. *Ceram Int*. 2017;43(6):4846–51. doi:10.1016/j.ceramint.2016.12.107.

3. Raju VSR. Synthesis of non-stoichiometric zinc ferrite for electromagnetic wave absorber applications. *Mater Sci Eng B*. 2017;224:88–92. doi:10.1016/j.mseb.2017.07.012.
4. Li L, Liu S, Lu L. Synthesis and significantly enhanced microwave absorption properties of cobalt ferrite hollow microspheres with protrusions/polythiophene composites. *J Alloys Compd*. 2017;722:158–65. doi:10.1016/j.jallcom.2017.06.029.
5. Zhang K, Gao X, Zhang Q, Chen H, Chen X. Fe_3O_4 nanoparticles decorated MWCNTs@C ferrite nanocomposites and their enhanced microwave absorption properties. *J Magn Magn Mater*. 2018;452:55–63. doi:10.1016/j.jmmm.2017.12.039.
6. Shen P, Luo J, Zuo Y, Yan Z, Zhang K. Effect of La-Ni substitution on structural, magnetic and microwave absorption properties of barium ferrite. *Ceram Int*. 2017;43(6):4846–51. doi:10.1016/j.ceramint.2016.12.107.
7. Kefeni KK, Msagati TAM, Mamba BB. Ferrite nanoparticles: Synthesis, characterisation and applications in electronic device. *Mater Sci Eng B*. 2017. doi:10.1016/j.mseb.2016.11.002.
8. Xie Y, Kocaefe D, Chen C, Kocaefe Y. Review of research on template methods in preparation of nanomaterials. *J Nanomater*. 2016. doi:10.1155/2016/2302595.
9. Mensah EE, Abbas Z, Azis RS, Khamis AM. Enhancement of complex permittivity and attenuation properties of recycled hematite (α-Fe_2O_3) using nanoparticles prepared via ball milling technique. *Materials (Basel)*. 2019;12(10). doi:10.3390/MA12101696.
10. Mensah EE, Abbas Z, Azis RS, Ibrahim NA, Khamis AM. Complex permittivity and microwave absorption properties of OPEFB fiber-polycaprolactone composites filled with recycled hematite (α-Fe_2O_3) nanoparticles. *Polymers (Basel)*. 2019;11(5). doi:10.3390/polym11050918.
11. Khamis AM, Abbas Z, Azis RS, Mensah EE, Alhaji IA. Fabrication and characterization of Fe_2O_3-OPEFB-PTFE nanocomposites for microwave shielding applications. *Polym Eng Sci*. 2022;62(11):3577–88. doi:10.1002/pen.26128.
12. Jensen FB, Kuperman WA, Porter MB, Schmidt H. *Computational Ocean Acoustics*. New York, NY: Springer; 2011. doi:10.1007/978-1-4419-8678-8.
13. Kim J, Song J, Jeong Y, Lee Y, Paik J, Kim W, Lee H. Fabrication of a high performance acoustic emission (AE) sensor to monitor and diagnose disturbances in HTS tapes and magnet systems. *Metals Mater Int*. 2010;16(1):115–9. doi:10.1007/s12540-010-0115-7.
14. Mensah EE, Abbas Z, Azis RS, Khamis AM. Enhancement of complex permittivity and attenuation properties of recycled hematite (α-Fe_2O_3) using nanoparticles prepared via ball milling technique. *Materials (Basel)*. 2019;12(10). doi:10.3390/MA12101696.
15. da Silva CP, dos Santos AV, Oliveira AS, da Guarda Souza MO. Synthesis of composites and study of the thermal behavior of sugarcane bagasse/iron nitrate mixtures in different proportions. *J Therm Anal Calorim*. 2018;131(1):611–20. doi:10.1007/s10973-017-6260-1.
16. Azis RS, Hashim M, Saiden NM, Daud N, Shahrani NMM. Study the iron environments of the steel waste product and its possible potential applications in

ferrites. *Adv Mater Res*. 2015;1109:295–9. doi:10.4028/www.scientific.net/amr.1109.295.
17. de Oliveira Aguiar V, Vieira Marques MF. Composites of polycaprolactone with cellulose fibers: Morphological and mechanical evaluation. *Macromol Symp*. 2016;367(1):101–12. doi:10.1002/masy.201500142.
18. Pozar DM. *Microwave Engineering*. 4th ed. USA: John Wiley and Sons Inc.; 2012.
19. Wang Q, Chen G. Effect of nanofillers on the dielectric properties of epoxy nanocomposites. *Adv Mater Res*. 2012;1(1):93–107.
20. Sharma P, Kanchan DK. Effect of nanofiller concentration on conductivity and dielectric properties of poly(ethylene oxide)-poly(methyl methacrylate) polymer electrolytes. *Polym Int*. 2014;63:290–5.
21. Pickering KL, Efendy MGA, Le TM. A review of recent developments in natural fibre composites and their mechanical performance. *Compos A Appl Sci Manuf*. 2016. doi:10.1016/j.compositesa.2015.08.038.